MOLECULAR ONCOLOGY 7 (2013) 130–142

available at www.sciencedirect.com

SciVerse ScienceDirect

www.elsevier.com/locate/molonc

Subtype-specific response to bevacizumab is reflected in the metabolome and transcriptome of breast cancer xenografts

Eldrid Borgan[a,b,c], *Evita M. Lindholm*[d], *Siver Moestue*[c], *Gunhild M. Mælandsmo*[d,e], *Ole Christian Lingjærde*[f], *Ingrid S. Gribbestad*[c], *Anne-Lise Børresen-Dale*[a,b], *Olav Engebraaten*[d,g], *Therese Sørlie*[a,h,*]

[a]*Department of Genetics, Institute for Cancer Research, Division for Cancer Medicine, Surgery and Transplantation, Oslo University Hospital, Norwegian Radium Hospital, P.O. Box 4953 Nydalen, 0424 Oslo, Norway*
[b]*Institute of Clinical Medicine, Faculty of Medicine, University of Oslo, Norway*
[c]*Department of Circulation and Medical Imaging, Norwegian University of Science and Technology (NTNU), 7491 Trondheim, Norway*
[d]*Department of Tumor Biology, Institute for Cancer Research, Division for Cancer Medicine, Surgery and Transplantation, Oslo University Hospital, Norwegian Radium Hospital, P.O. Box 4953 Nydalen, 0424 Oslo, Norway*
[e]*Department of Pharmacy, University of Tromsø, Tromsø, Norway*
[f]*Biomedical Research Group, Department of Informatics, University of Oslo, P.O. Box 1080 Blindern, 0316 Oslo, Norway*
[g]*Department of Oncology, Division for Cancer Medicine, Surgery and Transplantation, Oslo University Hospital Oslo, Norway*
[h]*Cancer Stem Cell Innovation Center, Oslo University Hospital, Norwegian Radium Hospital, Oslo, Norway*

ARTICLE INFO

Article history:
Received 15 August 2012
Accepted 15 October 2012
Available online 23 October 2012

Keywords:
Bevacizumab
Xenograft

ABSTRACT

Antiangiogenic therapy with bevacizumab has shown varying results in breast cancer clinical trials. Identifying robust biomarkers for selecting patients who may benefit from such treatment and for monitoring response is important for the future use of bevacizumab. Two established xenograft models representing basal-like and luminal-like breast cancer were used to study bevacizumab treatment response on the metabolic and gene expression levels. Tumor samples were obtained from mice treated with bevacizumab, doxorubicin or a combination of the two drugs, and high resolution magic angle spinning magnetic resonance spectroscopy and gene expression microarray analysis was performed.

Abbreviations: PFS, Progression Free Survival; OS, Overall Survival; FDA, Food and Drug Administration; tCHO, total Choline; MRS, Magnetic Resonance Spectroscopy; PCho, Phosphocholine; GPC, Glycerophosphocholine; HR MAS MRS, high resolution magic angle spinning magnetic resonance spectroscopy; SCID, Severe Combined Immuno Deficient; TSP, TrimethylSilyltetradeuteroPropionic acid; ERETIC, Electronic REference To access In vivo Concentrations; FE, Feature Extraction; IQR, Inter Quartile Range; GEO, Gene Expression Omnibus; ANOVA, Analysis Of Variance; FDR, False Discovery Rate; KEGG, Kyoto Encyclopedia of Genes and Genomes; GO, Gene Ontology.

* *Corresponding author*. Department of Genetics, Institute for Cancer Research, Division for Cancer Medicine, Surgery and Transplantation, Oslo University Hospital, Norwegian Radium Hospital, Postboks 4953 Nydalen, 0424 Oslo, Norway. Tel.: +47 22781364; fax: +47 22781395.

E-mail addresses: eldrid.borgan@gmail.com (E. Borgan), Evita.Lindholm@rr-research.no (E.M. Lindholm), siver.a.moestue@ntnu.no (S. Moestue), Gunhild.Mari.Malandsmo@rr-research.no (G.M. Mælandsmo), ole@ifi.uio.no (O.C. Lingjærde), ingrid.s.gribbestad@ntnu.no (I.S. Gribbestad), a.l.borresen-dale@medisin.uio.no (A.-L. Børresen-Dale), olav.engebraaten@gmail.com (O. Engebraaten), tsorlie@rr-research.no (T. Sørlie).

1574-7891/$ – see front matter
http://dx.doi.org/10.1016/j.molonc.2012.10.005

Breast cancer
Transcriptomics
Metabolomics

Combination treatment with bevacizumab showed the strongest growth inhibiting effect in basal-like tumors, and this was reflected by a significant change in the metabolomic and transcriptomic profiles. In the luminal-like xenografts, addition of bevacizumab did not improve the effect of doxorubicin. On the global transcriptomic level, the largest gene expression changes were observed for the most efficient treatment in both models. Glycerophosphocholine showed opposite response in the treated xenografts compared with untreated controls; lower in basal-like and higher in luminal-like tumors. Comparing combination therapy with doxorubicin monotherapy in basal-like xenografts, 14 genes showed significant differential expression, including very low density lipoprotein receptor (*VLDLR*) and hemoglobin, theta 1 (*HBQ1*). Bevacizumab-treated tumors were associated with a more hypoxic phenotype, while no evidence was found for associations between bevacizumab treatment and vascular invasion or tumor grade.

This study underlines the importance of characterizing biological differences between subtypes of breast cancer to identify personalized biomarkers for improved patient stratification and evaluation of response to therapy.

1. Introduction

Targeting tumor vasculature has evolved as an attractive strategy to treat solid tumors. One implemented strategy for several cancers is antiangiogenic treatment utilizing a VEGF targeting antibody (bevacizumab) (Braghiroli et al., 2012). Limited benefit in progression free survival (PFS) and lack of benefit in overall survival (OS) reported from clinical trials have raised questions about the relevance of bevacizumab for advanced breast cancer (Burstein, 2011). In 2010, FDA has revoked the breast cancer indication for bevacizumab. However, recent results have indicated that prolonged bevacizumab administration in metastatic breast cancer patients may give a benefit in OS (Bear et al., 2012; Smith et al., 2011; Von Minckwitz et al., 2012). The clinical utility of bevacizumab in breast cancer will depend on the identification of subgroups of patients who are likely to benefit from antiangiogenic therapy (Schneider and Sledge, Jr. 2011). Several potential biomarkers have been proposed, including VEGFR polymorphisms, and VEGF, PDGFR-β and VCAM1 expression (Schneider et al., 2008; Yang et al., 2008; Jubb et al., 2011; Baar et al., 2009), but none have been established as reproducible. Hence, the aim of this study was to investigate the biology of treatment response and possible resistance effects by combining metabolomics and transcriptomics of breast cancer xenograft models in order to identify response biomarker candidates for later verification in a clinical setting.

The tumor metabolome is known to be highly affected by extracellular factors such as the microenvironment, pH, oxygen, nutrients and drugs. Thus, metabolomic techniques have the potential to be more sensitive in monitoring treatment than other approaches such as measuring levels of RNA or proteins. Several metabolomic markers of treatment response have been suggested, including total choline (tCho), measured using *in vivo* MRS (Jagannathan et al., 2001; Meisamy et al., 2004), and phosphocholine (PCho), glycerophosphocholine (GPC) and lactate, measured using higher resolution MRS (Beloueche-Babari et al., 2010; Podo et al., 2011). High PCho levels or high PCho/GPC ratio with corresponding expression levels of genes involved in choline metabolism have been associated with malignancy and aggressiveness in both triple negative and ER positive breast cancer cell lines (Eliyahu et al., 2007; Glunde et al., 2004; Katz-Brull et al., 2002). On the other hand, high levels of GPC have been associated with ER negative tumors in studies of human breast carcinomas (Barzilai et al., 1991; Giskeodegard et al., 2010), suggesting that *in vitro* studies do not capture the complexity of tumor metabolism.

In vivo models are valuable tools for studying treatment response mechanisms since human carcinomas can be studied surrounded by a relevant microenvironment (Vargo-Gogola and Rosen, 2007). Two directly grafted orthotopic xenograft models representing basal-like and luminal-like breast cancer have previously been established and characterized at the transcriptomic and metabolomic levels (Bergamaschi et al., 2009; Lindholm et al., 2012; Moestue et al., 2010). The luminal-like model had a high PCho/GPC ratio while the basal-like model showed the opposite. The same differences were also found in clinical tumor samples, suggesting that these two models are relevant for studies of metabolism and treatment response in these two types of breast cancer (Moestue et al., 2010).

Recently, treatment studies in these models demonstrated that the basal-like model showed significantly improved response to bevacizumab and doxorubicin in combination compared with doxorubicin alone, while the luminal-like model responded equally well to doxorubicin with or without antiangiogenic therapy (Lindholm et al., 2012). Metabolomic and transcriptomic analysis of tumor tissue from these experiments was performed using high resolution magic angle spinning magnetic resonance spectroscopy (HR MAS MRS) and gene expression microarrays.

We demonstrate that GPC is a promising biomarker on the metabolomic level and that several gene transcripts are associated with bevacizumab responses in the responding basal-like tumors.

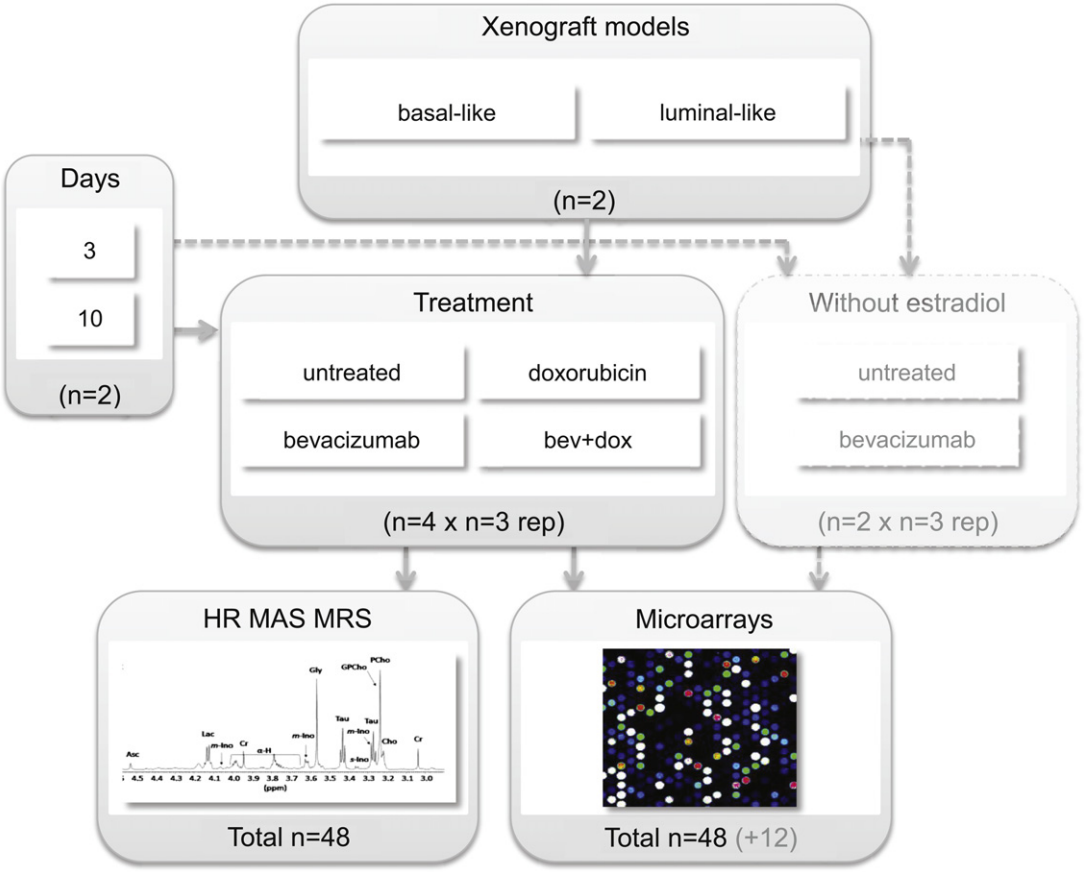

Figure 1 – Schematic illustration of the study design. Schematic illustration of the treatment experiments and metabolomic and transcriptomic analyses. Abbreviations: bev + dox: bevacizumab + doxorubicin; rep: replicates; HR MAS MRS: high resolution magic angle spinning magnetic resonance spectroscopy.

2. Material and methods

2.1. *Xenograft models and treatment*

Two orthotopic xenograft models, a basal-like (MAS98.12) and a luminal-like (MAS98.06), have been established by directly grafting human primary breast cancer tissue into SCID mice and serially transplanted, as previously described (Bergamaschi et al., 2009). An overview of the experimental procedure in the current work is illustrated in Figure 1. Animals from the two xenograft models were randomly assigned to different treatment groups after the tumor diameter reached approximately 5 mm. For each model, tumors were collected from animals that were untreated or treated repeatedly with bevacizumab at day 1, 4 and 7 (5 mg/kg), doxorubicin (8 mg/kg) at day 1 only, or a combination of the two therapies ($n = 6$ tumors for each group), as described in (Lindholm et al., 2012). Animals were sacrificed and tissue harvested at either day 3 or 10 after treatment, in triplicates within each treatment group, resulting in 24 tumor samples from each of the models. In addition, untreated and bevacizumab treated luminal-like xenografts not fed with estradiol were included for comparison ($n = 12$). Tumor tissue from all animals was stored in liquid nitrogen and separate tumor pieces were used for HR MAS MRS and gene expression microarray analysis. Out of the 48 samples from the estrogen fed animals analyzed with both experimental techniques, 33 were from the same tumor, 11 were from the same mouse but from different tumors (from bilateral implantations), and 4 were from different mice. The 12 tumors from animals not receiving estrogen supplement were included in the gene expression analysis for normalization purposes. All procedures and experiments involving animals were approved by the National Animal Research Authority and were conducted according to the regulations of the Federation of European Laboratory Animal Science Association (FELASA).

2.2. *HR MAS MRS experiments and data processing*

HR MAS MRS experiments and data preprocessing were performed on a Bruker Avance DRX600 spectrometer equipped with a 1H/13C HR MAS probe (Bruker BioSpin Corp.) as previously described (Moestue et al., 2010). Spectral assignments were performed based on a previous HR MAS MRS study of breast cancer lesions (Sitter et al., 2002). The regions representing the internal and electric standards TSP and ERETIC, as well as the metabolites creatine, choline, phosphocholine (PCho), glycerophosphocholine (GPC), taurine (Tau), glycine

(Gly), and lactate (Lac) were selected for quantification in all spectra. Peak areas were calculated by polynomial curve fitting (PeakFit v 4, Systat Software Inc) with a combination of Gaussian and Lorentzian line-shapes (Voigt function). Concentrations of tissue metabolites were calculated relative to the ERETIC signal as previously described (Moestue et al., 2010).

2.3. Gene expression microarray experiments and normalization

Total RNA from all 60 tumor pieces was extracted using the TRIzol reagent (Invitrogen) according to the manufacturer's protocol. Total RNA concentration was measured using NanoDrop (NanoDrop Technologies) and quality assessed using 2100 Bioanalyzer (Agilent Technologies). 700 ng total RNA was amplified, labeled using cy3-CTP and hybridized to one-color Agilent Technologies 4 × 44K Whole Human Genome Microarrays, as previously described (Moestue et al., 2010). Data were extracted from the scanned images using Feature Extraction (FE) software (Agilent Technologies) version 10.1.1.1 and protocol GE1-v5_10_Apr08 for mRNA and further processed and normalized using R (v2.10.1) and Bioconductor (Gentleman et al., 2004). Data from all samples were included in normalization and statistical analysis to increase power. Data were detrended for multiplicative effects and log2 transformed. Data from control probes, probes with inferior quality (feature outliers from FE) for more than 20 percent of the arrays, and probes that were flagged as present on less than 20 percent of the arrays were omitted from the analysis. The average value of duplicate probes was used to represent each unique probe. Missing data were imputed using k-nearest neighbors ($k = 10$) (Troyanskaya et al., 2001), and all data were quantile normalized. For transcripts (based on GeneName as provided by Agilent Technologies) represented by multiple different probes, the probe with the highest interquartile range (IQR) was chosen to represent each transcript. The normalized dataset included data for 28150 unique mRNA transcripts on 60 microarrays from the tumor biopsies; 24 from MAS98.12 animals, 24 from MAS98.06 animals fed with estradiol and 12 from MAS98.06 animals not fed with estradiol. The microarray data have been deposited in NCBI's Gene Expression Omnibus and are accessible through GEO Series accession number GSE37543 (http://www.ncbi.nlm.nih.gov/geo/query/acc.cgi?acc=GSE37543).

2.4. Statistical analysis

2.4.1. Analysis of metabolomic profiles

The quantified concentrations of the specific metabolites were used to assess whether any of these was affected by the treatments. Concentrations of each metabolite were modeled separately for each of the two xenografts using a two way ANOVA with interaction, the covariates treatment and days treated as factors. This analysis was used for pairwise comparisons between each treatment with no treatment at day 3 and day 10, respectively. For each day, the expected number of false positives is 42 * 0.05 = 2.1. The number of tests with nominal p-values <0.05 is 17.

2.4.2. Analysis of gene expression profiles

Gene expression data were analyzed for differences between treatments in the two xenograft models. Exploiting the factorial design of the experiments, the Bioconductor package Limma was used to model the expression levels of each transcript in the microarray data as a function of all combinations of the different days and treatments, equivalent of a two way ANOVA with interaction (Smyth, 2004). Data from the two xenograft models were modeled separately, and treatment and day were used as factors. An observed batch effect in the microarray data, corresponding to amplification date, was corrected for in the model by using the blocking factor implemented in Limma (Smyth et al., 2005). All pairwise comparisons between treated and untreated xenografts from the same day were analyzed by relevant contrasts to the model as described by Smyth (Smyth, 2011). Additionally, the combination treatment was compared with doxorubicin monotherapy. The test statistics were Empirical Bayes modified and p-values were corrected for multiple testing using Benjamini Hochberg false discovery rate (FDR) for each pairwise comparison separately (Benjamini and Hochberg, 1995; Smyth, 2004). This analysis was performed on all gene transcripts and on a gene set of 105 genes representing phospholipid metabolism (involved in KEGG glycerophospholipid pathway, choline transport, or choline and glycine metabolism), as previously described (Moestue et al., 2010). To analyze whether any biological processes were enriched among the genes most differentially expressed between treated and untreated xenografts, GOrilla was used (Eden et al., 2009). For each comparison, lists of all 28150 transcripts in the microarray data were ranked according to fold change and analyzed for GO-term enrichment towards the top of the lists.

2.4.3. Using gene expression signatures as surrogate measures

Published microarray based gene expression signatures including genomic grade index (GGI) (Sotiriou et al., 2006), a hypoxia classifier (Chi et al., 2006) and a vascular invasion signature (Mannelqvist et al., 2011) were used to study differences in specific biological features in relation to bevacizumab treatment effects and possible induced resistance. Using scores from each of these signatures, comparisons between the two xenograft models and between the treatments were performed using ANOVA (similar to the analysis for assessing differences in metabolite concentrations). The original probes in the GGI (Affymetrix ID) and hypoxia gene signatures (Clone IDs) were matched to Agilent Probe IDs using the R-package BiomaRt (Durinck et al., 2005), while the genes in the vascular invasion signature were matched by gene symbol directly. To analyze differences in aggressiveness between the untreated basal-like and luminal-like tumors as well as between treated and untreated tumors for each of the two models, the gene expression based GGI was used as a surrogate measure. Raw GGI scores were calculated by using a weighted average of the expression levels of genes shown to differentiate between grade I and III breast carcinomas (Sotiriou et al., 2006) and used directly. For hypoxia assessment in the tumor samples, a set of genes induced by hypoxia in cultured epithelial cells were investigated (Chi et al., 2006). For each probe for each sample, the median expression value across all samples was

subtracted. Next, the hypoxia score was defined by calculating the median expression of the hypoxia related genes for each sample. A recently published vascular invasion signature was used as surrogate marker for vascular invasion of tumor epithelial cells (Mannelqvist et al., 2011). This gene signature represents differences in gene expression between vascular invasion positive and negative endometrial tumors, based on staining for presence of tumor cells in blood vessels. Data for the selected genes were mean centered across all samples, and the published log fold change of each gene was analyzed for nonzero correlations with the expression of the matched genes for each xenograft sample. The correlation coefficients were used as scores to compare vascular invasion between the xenograft models and treatments.

2.4.4. *Analysis of phospholipid metabolism gene expression in a patient cohort*

To assess whether the distinct expression patterns of genes involved in phospholipid metabolism previously observed in the two xenograft models (Moestue et al., 2010) are representative of basal-like and luminal-like cancer, a microarray dataset from a patient cohort of 115 breast carcinomas was analyzed (Enerly et al., 2011). Since the patient and xenograft microarray data were from the same platform (Agilent Technologies 4 × 44K Whole Human Genome Microarrays), the probes representing the 105 phospholipid metabolism genes were exactly matched between the two datasets. The assigned intrinsic subtypes of the patient tumors were used to select the 16 basal-like tumors and 61 luminal tumors in the dataset (including both luminal A and luminal B). Data were centered across genes and a heatmap was generated by clustering of the 105 genes and 77 samples using Pearson's correlation and average linkage. Limma was used to test for differences between the two groups in the patient data, and generated (modified) *t*-statistics were compared with those from the xenograft data (as previously published (Moestue et al., 2010)) using Pearson's correlation test.

3. Results

3.1. *Metabolomic response to treatment*

Quantified metabolite concentrations were used to analyze differences in Cho, GPC, PCho, tCho, Tau, Cre, Gly and Lac between treated and untreated tumors from both models (See Supplementary Figure 1). The basal-like xenograft represented a bevacizumab responder while the luminal-like xenograft represented a non-responder to this drug. Therefore, changes observed after treatment with bevacizumab in basal-like and not in luminal-like tumors were of particular interest as these could have the potential of being used in treatment monitoring. Indeed, GPC is potentially such a marker, as it showed opposite patterns of response to treatment in the two differently responding xenograft models (Figure 2). In basal-like tumors, GPC concentrations were significantly lower after any of the three treatment modalities at day 10, and there was a similar trend at day 3. This was in contrast to luminal-like tumors, where GPC concentrations were significantly *higher* in the doxorubicin and combination treated tumors compared with untreated tumors at day 10 and no significant changes were observed for bevacizumab monotherapy, indicating that this response is triggered by doxorubicin treatment. PCho on the other hand, showed either no change in concentrations or tended to increase in treated animals of both models (Figure 2). In the basal like model, there was no change in tCho, in contrast to the luminal-like model demonstrating a significant increase after the combination treatment compared with no treatment. Thus, the value of tCho as a response marker by using *in vivo* MRS may be reduced due to these differences in patterns of choline derivatives between tumor subgroups. Table 1 summarizes all metabolites that displayed either higher or lower levels after the three different treatment regimes at day 10. None of the other metabolites demonstrated predictive value.

3.2. *Gene expression response to the most efficient treatment*

The most efficient treatment, measured as growth delay in each of the two models, was associated with the largest magnitude of gene expression changes at day 10 (Figure 3). Significantly enriched biological processes were also found among the most differentially expressed genes. For the basal-like model, the largest transcriptional response was seen in tumors from animals given the combination therapy, and 40 transcripts showed significantly different levels compared with untreated tumors; 38 at higher expression levels (the most significant being *HOXB13*, *PPP1R3C*, *TMEM45A*) and 2 genes at lower expression levels (*SLC2A12* and *KRT5*) (Figure 3A and Supplementary Table 1). Furthermore, when comparing combination treated with doxorubicin only treated basal-like tumors, 14 transcripts showed significantly different expression; 8 higher expressed, the most significant being *VLDLR*, *PPFIA4* and *MCHR1*, and 6 lower expressed, the most significant being *DAB1*, *HBQ1* and *ACCN1* (Table 2). Five of these genes (*VLDLR*, *PPFIA4*, *MCHR1*, *PPP1R3C* and *CHI3L1*) were overlapping with the 40 genes which showed significantly different expression between combination treatment and no treatment (indicated in bold in Figure 3A). The GO-term "muscle contraction" was enriched among the transcripts higher expressed in the combination treated versus both the doxorubicin only treated and untreated basal-like tumors (Supplementary Table 2). In addition, several immune process related GO-terms such as "immune response", "inflammatory response" and "response to cytokine stimulus" were enriched among the transcripts that were lower expressed in the combination treated when compared with doxorubicin treated basal-like tumors. However, expression changes of such genes in xenograft tumors are difficult to interpret, since the host animals are immunocompromised.

For the luminal-like model, the largest response was observed in tumors treated with doxorubicin monotherapy, and 380 transcripts showed significantly different expression compared with the untreated animals. Of these, 201 were higher expressed, the most significant being *EGF*, *RARRES3* and *CAPSL*. Lower expression levels were seen in 179 genes, the most significant being *HBA2*, *HBA1* and *KCNK5* (the top 100 genes are shown in Figure 3B and the full list is given in Supplementary

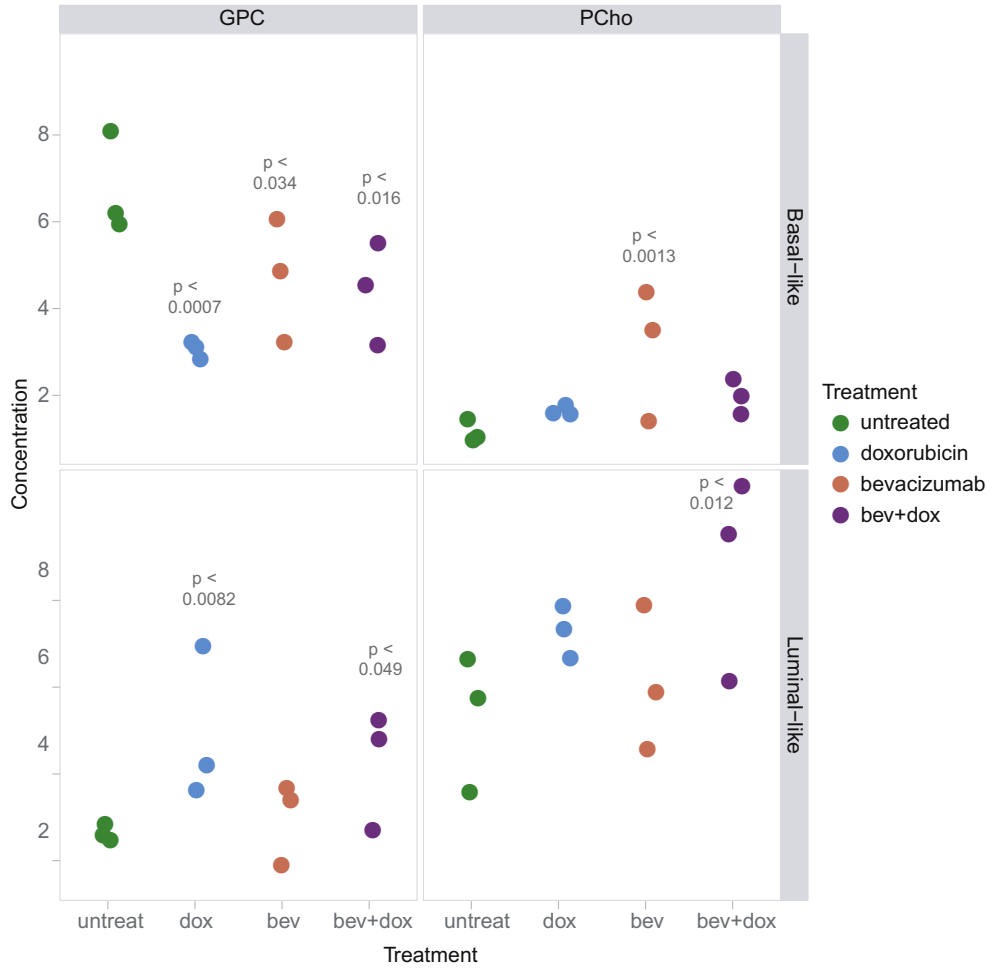

Figure 2 – Changes in glycerophosphocholine and phosphocholine reflect response to treatment. Concentrations of glycerophosphocholine (GPC) and phosphocholine (PCho) at day 10 plotted for each xenograft model and colored according to treatment ($n = 3$ animals per group). Significant differences in mean concentration between treated and untreated tumors are indicated with the associated nominal p-values. Abbreviations: bev + dox: bevacizumab + doxorubicin.

Table 3). In doxorubicin treated versus untreated luminal-like tumors, GO-terms such as "type I interferon-mediated signaling pathway", "muscle contraction" and "muscle filament sliding" were significantly enriched among the transcripts that were higher expressed. Among the transcripts that were lower expressed, the terms "DNA replication", "DNA strand elongation involved in DNA replication" and "ncRNA processing" were significantly enriched (Supplementary Table 2), which is in agreement with the proposed mechanism of doxorubicin of targeting topoisomerase II.

3.3. *Gene expression signatures as surrogate markers for adaptive resistance*

Evasive or adaptive resistance mechanisms to antiangiogenic treatment have been suggested, such as increased aggressiveness/invasiveness or recruitment of bone marrow-derived cells due to increased hypoxia and lack of nutrients (Bergers and Hanahan, 2008). The published gene expression signatures GGI (Sotiriou et al., 2006), hypoxia (Chi et al., 2006) and vascular invasion (Mannelqvist et al., 2011) were used as surrogate markers for the extent of aggressiveness, hypoxia and vascular invasion by tumor epithelial cells, respectively.

A score for each of the three signatures was calculated for each sample. These scores were compared between the treatments and no treatment at each day (Figure 4). Gene signature scores were also compared between the two models using the untreated tumors (results not shown). Lower GGI scores were observed after treatment with combination of bevacizumab and doxorubicin in both xenograft models at day 10, and a significant decrease was also observed for the basal-like tumors after bevacizumab monotherapy. This suggests that bevacizumab treatment reduced some aggressive features of these tumors. There was not significant evidence of differences in GGI between the two untreated xenograft models. Notably, a significantly higher GGI was observed in the doxorubicin treated basal-like tumors at day 3 compared with untreated tumors. Using the hypoxia gene signature, hypoxia scores increased in the basal-like model after

Table 1 – Metabolomic response to treatment. Overview of metabolites that displayed significantly (nominal p-values < 0.05) different mean concentrations in treated compared with untreated xenograft models at day 10. Arrows indicate whether the concentration of each metabolite was higher (↑) or lower (↓) after treatment.

Xenograft	Metabolites	Doxorubicin	Bevacizumab	Bevacizumab + doxorubicin
Basal-like	Cholines	GPC[a]↓***, tCho[b]↓*	Pcho[c]↑*, GPC↓*	GPC↓*
	Other metabolites	Gly↓***, Cre[e]↓***, Tau[d]↓*	Gly[f]↓*, Cre↓**, Tau↓*	
Luminal-like	Cholines	GPC↑**, tCho↑*		PCho↑*, GPC↑*, tCho↑**
	Other metabolites			Tau↓*

*$p < 0.05$, **$p < 0.01$, ***$p < 0.001$.
a GPC: glycerophosphocholine.
b tCho: total choline.
c PCho: phosphocholine.
d Tau: taurine.
e Cre: creatine.
f Gly: glycine.

treatment with either bevacizumab or the combination treatment at both day 3 and 10. A significant increase was also observed in bevacizumab treated luminal-like tumors at day 3. The untreated luminal-like tumors had significantly higher hypoxia scores than the untreated basal-like tumors, suggesting that the luminal-like tumors were more hypoxic than the basal-like tumors. When comparing vascular invasion gene signature scores between the two models, basal-like tumors showed significantly higher baseline scores. While no significant differences in vascular invasion scores between treatments were observed for the basal-like model, significantly higher scores were observed for luminal-like tumors treated with doxorubicin and combination treatment at day 10. This result suggests that vascular invasion could be increased in the doxorubicin treated luminal-like tumors, while there is no evidence for bevacizumab inducing such an effect.

3.4. *Comparison of phospholipid metabolism between xenografts and human carcinomas by means of gene expression*

In a previous study, we showed that genes involved in choline transport, phospholipid metabolism, and glycine metabolism were differentially expressed between the basal-like and luminal-like xenograft models, and that levels of expression corresponded to metabolomic changes (Moestue et al., 2010). Using these same genes to analyze differences between treated and untreated tumors, the *LCAT* gene (encoding the enzyme lecithin-cholesterol acyltransferase) showed significantly higher levels of expression in combination treated versus untreated basal-like tumors at day 10. There were no other significant changes in expression of genes involved in phospholipid metabolism. The observed metabolomic responses of choline derivatives may reflect intrinsic differences in phospholipid metabolism between the models. To assess whether the metabolic phenotypes of the xenograft models are intrinsic properties of basal-like and luminal-like tumors on the gene expression level, a human breast tumor microarray dataset was used to compare expression differences of genes involved in phospholipid metabolism between these two biologically distinct subgroups of breast cancer (Supplementary Figure 2A). A clustering analysis revealed great similarity between basal-like tumors, while the luminal-like tumors were more heterogeneous in their expression of genes involved in phospholipid metabolism. Analyses of differential expression of these genes between basal-like and luminal-like tumors were compared between human and xenograft tumors. The correlation between these two analyses was found to be significant (rho = 0.34, p-value $< 4.1 \times 10^{-4}$) (Supplementary Figure 2B and C). The most significant differences in gene expression observed both in the xenograft and human basal-like versus luminal-like tumors included higher expression of *PLA2G4A*, *PLCG2* and *AGPAT4*; and lower expression of *GPD1L*, *PLCD4* and *ETNK2*.

4. Discussion

Antiangiogenic therapy such as bevacizumab may be more efficient in certain subgroups of breast cancer. To exploit the potential of bevacizumab as a breast cancer drug, individualized biomarkers are needed to select patients and assess treatment response. Metabolomic biomarkers are especially attractive because they have the potential of being measured *in vivo* allowing treatment monitoring and adaptation of given therapy according to response. In the present study, the metabolite with highest potential as a biomarker for monitoring response to bevacizumab was GPC which showed opposite response patterns in the two xenografts; lower in the treated basal-like tumors and higher in treated luminal-like tumors compared with untreated controls. PCho on the other hand, showed either no difference or an increase in concentration in both models. This underlines the importance of characterizing subtypes of breast cancer separately when evaluating response markers for treatment monitoring. Clinical 1-H *in vivo* MRS of breast tumors detects tCho which is the sum of GPC, PCho and Cho signals. Opposite behavior of GPC and PCho in response to treatment, as observed using *ex vivo* HR MAS MRS for the basal-like tumors, may impact the utility of tCho as a response marker. However, with increasing field strengths and the possibility of implementing 31-P coils in clinical magnets, the GPC and PCho peaks could be separated in the spectra obtained *in vivo* (Morse et al., 2007). Thus, metabolomic biomarkers such as GPC could in the future be measured non-invasively and potentially used both as

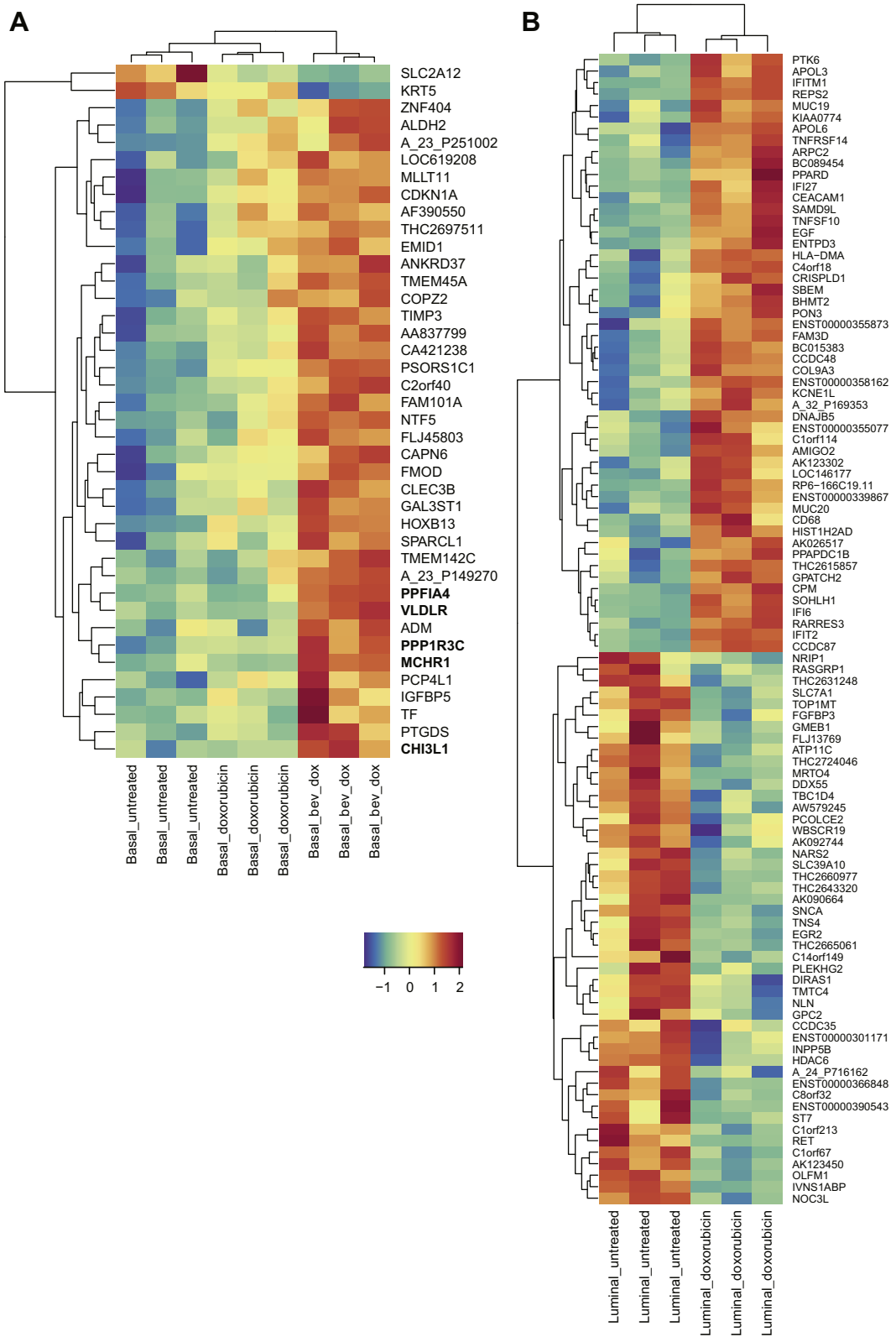

Figure 3 – Subtype-specific response to treatment reflected in transcriptomic profiles. Heatmaps of significantly differentially expressed genes (FDR < 0.05) at day 10 between untreated xenografts and xenografts given the most efficient treatment for each model: (A) combination treatment for basal-like and (B) doxorubicin for luminal-like xenografts (only the top 100 transcripts are shown). Each gene was mean centered and clustering of samples and genes was performed using Euclidian distance and complete linkage. The color coding is based on scaled expression values where each gene is scaled to have mean zero and standard deviation one. Transcripts that were also significantly differentially expressed when comparing combination treated with doxorubicin treated basal-like tumors (Listed in Table 2) are indicated with bold gene symbols in A. Abbreviations: bev_dox: bevacizumab + doxorubicin.

Table 2 – Additional transcriptomic response to bevacizumab in basal-like xenografts. Transcripts with significant (FDR < 0.05) difference in mean expression levels between basal-like tumors that received combination of bevacizumab and doxorubicin compared with those that received doxorubicin monotherapy.

Probe name	Gene name	Description	logFC[a]	t	p-value	FDR[b]
Higher expression levels in combination treated tumors						
A_23_P43476	VLDLR	Very low density lipoprotein receptor, transcript variant 1	1.4	7.8	1.7E-07	0.0047
A_23_P420692	PPFIA4	Protein tyrosine phosphatase, receptor type, f polypeptide (PTPRF), interacting protein (liprin), alpha 4	1.0	6.6	1.9E-06	0.013
A_23_P139166	CB959193	CB959193 AGENCOURT_13778270 NIH_MGC_184 cDNA clone IMAGE:30351353 5′	1.9	6.2	4.7E-06	0.019
A_23_P211543	MCHR1	Melanin-concentrating hormone receptor 1	0.8	6.0	6.2E-06	0.022
A_23_P35414	PPP1R3C	Protein phosphatase 1, regulatory (inhibitor) subunit 3C	1.6	5.9	8.2E-06	0.026
A_23_P137665	CHI3L1	Chitinase 3-like 1 (cartilage glycoprotein-39)	0.93	5.8	9.7E-06	0.027
A_32_P128586	DA727827	DA727827 NT2RM1 cDNA clone NT2RM1001124 5′	0.86	5.8	1.2E-05	0.029
A_23_P117851	CPLX3	Complexin 3	0.93	5.6	1.6E-05	0.032
Lower expression levels rin combination treated tumors levels						
A_23_P23850	DAB1	Disabled homolog 1 (drosophila)	−1.7	−6.6	1.9E-06	0.013
A_23_P49254	HBQ1	Hemoglobin, theta 1	−1.6	−6.7	1.5E-06	0.013
A_32_P159612	ACCN1	Amiloride-sensitive cation channel 1, neuronal (degenerin)	−1.7	−6.4	3.1E-06	0.017
A_24_P416097	ENST00000336999	UNC45 homolog A (UNC-45A) (Smooth muscle cell-associated protein 1)	−1.2	−6.3	3.6E-06	0.017
A_24_P75190	HBD	Hemoglobin, delta	−2.0	−5.7	1.3E-05	0.030
A_23_P29939	SNCA	Synuclein, alpha (non A4 component of amyloid precursor), transcript variant NACP112	−2.0	−5.7	1.4E-05	0.030

a logFC: log2 fold change.
b FDR: false discovery rate.

a biomarker for selecting patients for bevacizumab treatment and for monitoring response to treatment.

On the gene expression level, this study suggests that the most significant gene expression changes occur in tumors which benefit the most from a given treatment, i.e. the combination of bevacizumab and doxorubicin for basal-like and doxorubicin monotherapy for luminal-like tumors. A similar trend was also found tumors at the proteomic level, i.e. the most effective treatment was linked to higher kinase activity at day 10 (Lindholm et al., 2012). The transcripts expressed at significantly different levels between the combination and doxorubicin treated tumors in the basal-like xenograft model (Table 2) are particularly interesting since these may suggest biological mechanisms for the additional effect of bevacizumab. Five of these genes were also significantly higher expressed in the bevacizumab and doxorubicin combination treated compared with untreated tumors, including *VLDLR* and *CHI3L1* which have both previously been associated with angiogenesis (Oganesian et al., 2008; Saidi et al., 2008; Nishikawa and Millis, 2003). Of the transcripts which showed reduced expression after the combination treatment compared with doxorubicin, two hemoglobins (*HBQ1* and *HBD*) were represented. It could be speculated that the genes showing higher expression may represent adaptive resistance processes while the lower expressed genes could represent changes in composition of different cell types in the tumors due to the antiangiogenic effects of bevacizumab. It should however be noted that all measurements in this study are based on bulk tumors from the mice, using human specific microarrays, and cross hybridization of mouse specific genes from the stromal compartment cannot be ruled out.

Focusing solely on genes involved in phospholipid metabolism (Moestue et al., 2010), *LCAT* was the only gene found to be significantly differentially expressed in response to treatment. LCAT has both cholesterol and phosphatidylcholine (PtdCho, also called lecithin) acetyltransferase activity and may thus catalyze the same reaction as phospholipase A2. The increase in expression of *LCAT* in combination treated basal-like tumors may be counterintuitive to the decrease in GPC as measured by HR MAS MRS. However, the increase in *LCAT* levels could e.g. be due to feedback mechanisms rather than exerting a direct effect on the levels of GPC. The apparent lack of transcriptional response of genes involved in phospholipid metabolism shows that the observed responses in choline derivatives are not necessarily coupled to changes at the gene expression level. This may be because changes in

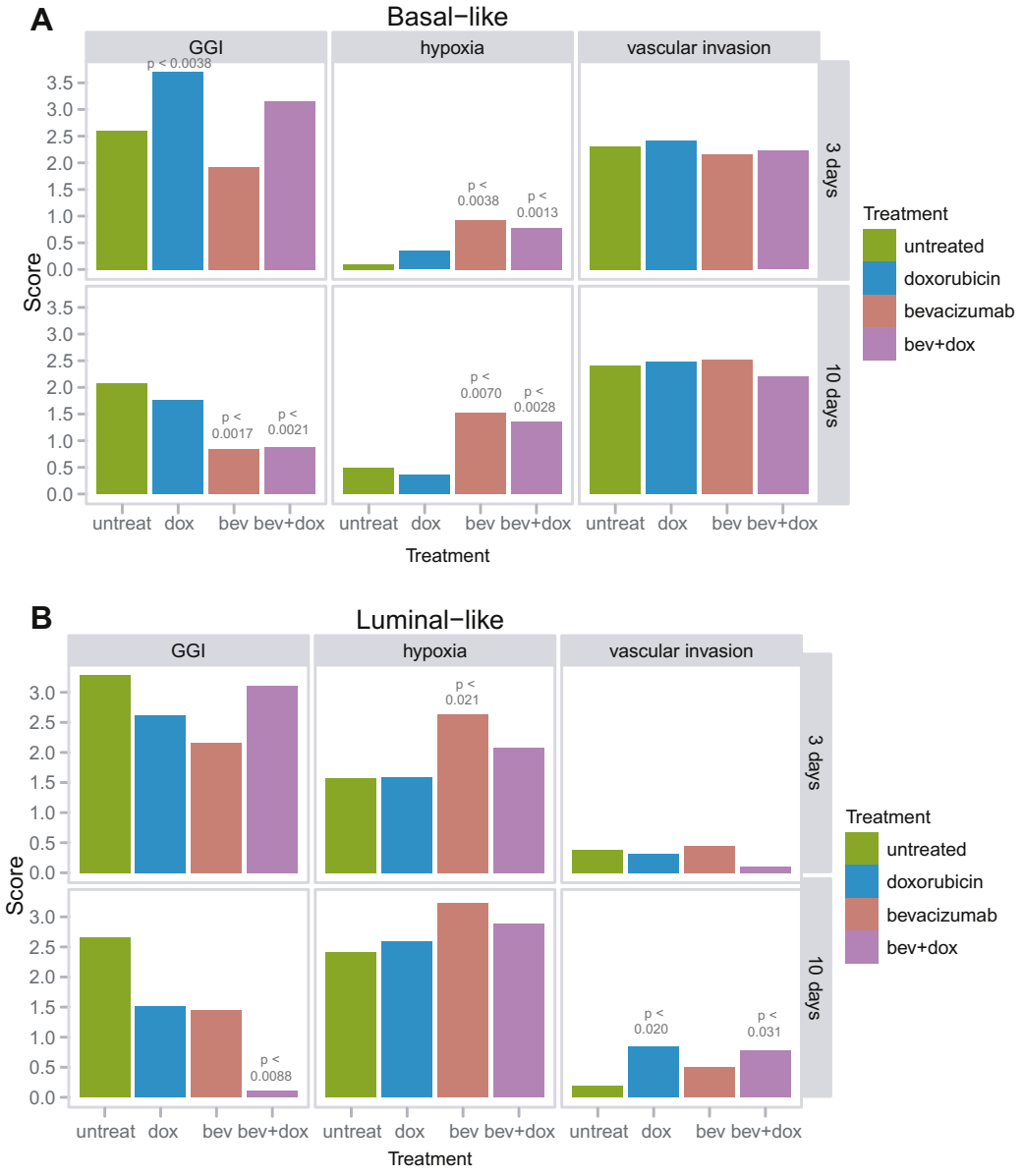

Figure 4 – Changes in gene expression signatures after treatment. Barplots of scores from the three gene expression signatures genomic grade index (GGI) (Sotiriou et al., 2006), hypoxia (Chi et al., 2006), and vascular invasion (Mannelqvist et al., 2011) for A) basal-like and B) luminal-like xenograft models (each bar represents $n = 3$ replicates). The scores were scaled across all samples to make them comparable and significant differences in mean scores between treated and untreated tumors at each day are indicated with the associated nominal p-values. Abbreviations: bev + dox: bevacizumab + doxorubicin.

enzymatic activity are regulated at the post-translational level. Also, the distinct gene expression patterns of phospholipid metabolism genes found in the untreated basal-like and luminal-like xenografts correlated with those of human breast tumors (Supplementary Figure 2), supporting that the differences in phospholipid metabolism may be an intrinsic characteristic of basal-like and luminal-like breast cancer. Interestingly, the PLA2 coding gene *PLA2G4A* was one of the most significantly differentially expressed genes between basal-like (higher) and luminal-like (lower) for both xenografts and human tumors. *PLA2G4A* has been reported to be lower expressed in breast cancer cells concomitant with low GPC levels compared with normal epithelial breast cells (Glunde et al., 2004), and has been found to be inversely correlated with *ESR1* expression in breast cancer cell lines and human breast carcinomas (Caiazza et al., 2011). Thus, targeting *PLA2G4A* could perhaps be an interesting approach in treatment of basal-like cancers.

Bevacizumab associated changes in expression of genes involved in biological processes associated with adaptive treatment resistance are of particular interest in light of the limited success of bevacizumab in breast cancer clinical trials. Two different modes of resistance to antiangiogenic therapy have been suggested (Bergers and Hanahan, 2008), and

following these definitions the luminal-like xenograft model may represent an intrinsic non-responder while the basal-like xenograft model may represent a responder which could develop adaptive resistance. The observed bevacizumab associated decrease in genomic grade index (GGI) for both models (Figure 4) is contradictory to claims that antiangiogenic therapy may increase tumor aggressiveness (Kerbel, 2009; Paez-Ribes et al., 2009). However, bevacizumab associated increases in hypoxia gene signature scores were observed, especially in the basal-like xenograft model (Figure 4). Increased hypoxia has been linked to invasiveness and metastasis (Young and Hill, 1990), and has been proposed to induce adaptive resistance to antiangiogenic therapies (Du et al., 2008). It is worth noting that aldehyde dehydrogenase 2 family (*ALDH2*), which was among the most significantly higher expressed genes after combination treatment in basal-like xenografts (Figure 3), has in addition to being involved in many metabolic pathways been linked to hypoxia (Milosevic et al., 2007).

A possible indication of treatment induced invasiveness was enrichment of the GO-term "muscle contraction" (including genes such as myosin and actin) when comparing the combination treated with untreated basal-like tumors or with doxorubicin only treated tumors (Supplementary Table 2). A suggested adaptive resistance mechanism is in fact tumor cell migration to more vascularized areas (Rubenstein et al., 2000; Du et al., 2008). However, similar GO-terms were also enriched among genes with higher expression after doxorubicin monotherapy of the luminal-like xenografts, contradicting that this change is associated specifically with bevacizumab treatment. Finally, the limitations of this study, including only two xenograft models with three replicates in each treatment group at each day should be kept in mind. However, these models have been shown to be representative for basal-like and luminal-like breast cancer, and the results presented in this study are thus likely to be relevant for these subtypes of breast cancer.

In summary, this study has highlighted how subtype specific response to bevacizumab was reflected on the metabolomic and transcriptomic levels. The biological connection between the molecular response at the metabolomic and transcriptomic level was not evident, which underlines the complementary nature of the information retrieved from these two types of analyses. Importantly, the results from this study support the necessity of patient stratification with respect to biologically relevant subgroups when searching for biomarkers in preclinical as well as clinical breast cancer trials. Results from different clinical trials of bevacizumab in non-metastatic breast cancer, have reported that both ER positive cancers (Bear et al., 2012) and triple negative cancers (Von Minckwitz et al., 2012) may benefit from the addition of bevacizumab to chemotherapy. Clearly, biological and molecular features apart from the more traditional histopathological subtype definition may determine whether a tumor is responsive to bevacizumab and in which combinatorial regimen an optimal efficacy may be reached. Also, biomarkers with the potential to predict or monitor treatment response may be found across subtypes. Thus, new xenograft models representing the tumor heterogeneity of basal-like and luminal-like cancers and carefully planned clinical trials will be important for investigating the biology of bevacizumab response in breast cancer.

Acknowledgments

This work was supported by the Norwegian Research Council (163027 to TS, and FUGE project 183379 and 183621), funds from The South-Eastern Norway Regional Health Authority and a generous donation from Monica Nordal memorial fund to OE.

The authors thank Hilde Johnsen for technical support, Xi Zhao for sharing her expertise in R and for cross-platform matching of gene signatures, and Lars Akslen for assistance with the vascular signature analysis.

Appendix A. Supplementary data

Supplementary data related to this article can be found at http://dx.doi.org/10.1016/j.molonc.2012.10.005.

REFERENCES

Baar, J., Silverman, P., Lyons, J., Fu, P., Abdul-Karim, F., Ziats, N., Wasman, J., Hartman, P., Jesberger, J., Dumadag, L., Hohler, E., Leeming, R., Shenk, R., Chen, H., McCrae, K., Dowlati, A., Remick, S.C., Overmoyer, B., 2009. A vasculature-targeting regimen of preoperative docetaxel with or without bevacizumab for locally advanced breast cancer: impact on angiogenic biomarkers. Clinical Cancer Research 15, 3583–3590.

Barzilai, A., Horowitz, A., Geier, A., Degani, H., 1991. Phosphate metabolites and steroid hormone receptors of benign and malignant breast tumors. A Nuclear Magnetic Resonance study. Cancer 67, 2919–2925.

Bear, H.D., Tang, G., Rastogi, P., Geyer Jr., C.E., Robidoux, A., Atkins, J.N., Baez-Diaz, L., Brufsky, A.M., Mehta, R.S., Fehrenbacher, L., Young, J.A., Senecal, F.M., Gaur, R., Margolese, R.G., Adams, P.T., Gross, H.M., Costantino, J.P., Swain, S.M., Mamounas, E.P., Wolmark, N., 2012. Bevacizumab added to neoadjuvant chemotherapy for breast cancer. The New England Journal of Medicine 366, 310–320.

Beloueche-Babari, M., Chung, Y.L., Al-Saffar, N.M., Falck-Miniotis, M., Leach, M.O., 2010. Metabolic assessment of the action of targeted cancer therapeutics using magnetic resonance spectroscopy. The British Journal of Cancer 102, 1–7.

Benjamini, Y., Hochberg, Y., 1995. Controlling the false discovery rate: a practical and powerful approach to multiple testing. Journal of the Royal Statistical Society. Series B (Methodological) 57, 289–300.

Bergamaschi, A., Hjortland, G.O., Triulzi, T., Sørlie, T., Johnsen, H., Ree, A.H., Russnes, H.G., Tronnes, S., Maelandsmo, G.M., Fodstad, O., Borresen-Dale, A.L., Engebraaten, O., 2009. Molecular profiling and characterization of luminal-like and basal-like in vivo breast cancer xenograft models. Molecular Oncology 3, 469–482.

Bergers, G., Hanahan, D., 2008. Modes of resistance to anti-angiogenic therapy. Nature Reviews Cancer 8, 592–603.

Braghiroli, M.I., Sabbaga, J., Hoff, P.M., 2012. Bevacizumab: overview of the literature. Expert Review of Anticancer Therapy 12, 567–580.

Burstein, H.J., 2011. Bevacizumab for advanced breast cancer: all tied up with a RIBBON? Journal of Clinical Oncology 29, 1232–1235.

Caiazza, F., McCarthy, N.S., Young, L., Hill, A.D., Harvey, B.J., Thomas, W., 2011. Cytosolic phospholipase A2-alpha expression in breast cancer is associated with EGFR expression and correlates with an adverse prognosis in luminal tumours. British Journal of Cancer 104, 338–344.

Chi, J.T., Wang, Z., Nuyten, D.S., Rodriguez, E.H., Schaner, M.E., Salim, A., Wang, Y., Kristensen, G.B., Helland, A., Borresen-Dale, A.L., Giaccia, A., Longaker, M.T., Hastie, T., Yang, G.P., van de Vijver, M.J., Brown, P.O., 2006. Gene expression programs in response to hypoxia: cell type specificity and prognostic significance in human cancers. PLoS Medicine 3, e47.

Du, R., Lu, K.V., Petritsch, C., Liu, P., Ganss, R., Passegue, E., Song, H., Vandenberg, S., Johnson, R.S., Werb, Z., Bergers, G., 2008. HIF1alpha induces the recruitment of bone marrow-derived vascular modulatory cells to regulate tumor angiogenesis and invasion. Cancer Cell 13, 206–220.

Durinck, S., Moreau, Y., Kasprzyk, A., Davis, S., De Moor, B., Brazma, A., Huber, W., 2005. BioMart and Bioconductor: a powerful link between biological databases and microarray data analysis. Bioinformatics 21, 3439–3440.

Eden, E., Navon, R., Steinfeld, I., Lipson, D., Yakhini, Z., 2009. GOrilla: a tool for discovery and visualization of enriched GO terms in ranked gene lists. BMC Bioinformatics 10, 48.

Eliyahu, G., Kreizman, T., Degani, H., 2007. Phosphocholine as a biomarker of breast cancer: molecular and biochemical studies. International Journal of Cancer 120, 1721–1730.

Enerly, E., Steinfeld, I., Kleivi, K., Leivonen, S.K., Aure, M.R., Russnes, H.G., Ronneberg, J.A., Johnsen, H., Navon, R., Rodland, E., Makela, R., Naume, B., Perala, M., Kallioniemi, O., Kristensen, V.N., Yakhini, Z., Borresen-Dale, A.L., 2011. miRNA-mRNA integrated analysis reveals roles for miRNAs in primary breast tumors. PLoS One 6, e16915.

Gentleman, R.C., Carey, V.J., Bates, D.M., Bolstad, B., Dettling, M., Dudoit, S., Ellis, B., Gautier, L., Ge, Y., Gentry, J., Hornik, K., Hothorn, T., Huber, W., Iacus, S., Irizarry, R., Leisch, F., Li, C., Maechler, M., Rossini, A.J., Sawitzki, G., Smith, C., Smyth, G., Tierney, L., Yang, J.Y., Zhang, J., 2004. Bioconductor: open software development for computational biology and bioinformatics. Genome Biology 5, R80.

Giskeodegard, G.F., Grinde, M.T., Sitter, B., Axelson, D.E., Lundgren, S., Fjosne, H.E., Dahl, S., Gribbestad, I.S., Bathen, T.F., 2010. Multivariate modeling and prediction of breast cancer prognostic factors using MR metabolomics. Journal of Proteome Research 9, 972–979.

Glunde, K., Jie, C., Bhujwalla, Z.M., 2004. Molecular causes of the aberrant choline phospholipid metabolism in breast cancer. Cancer Research 64, 4270–4276.

Jagannathan, N.R., Kumar, M., Seenu, V., Coshic, O., Dwivedi, S.N., Julka, P.K., Srivastava, A., Rath, G.K., 2001. Evaluation of total choline from in-vivo volume localized proton MR spectroscopy and its response to neoadjuvant chemotherapy in locally advanced breast cancer. British Journal of Cancer 84, 1016–1022.

Jubb, A.M., Miller, K.D., Rugo, H.S., Harris, A.L., Chen, D., Reimann, J.D., Cobleigh, M.A., Schmidt, M., Langmuir, V.K., Hillan, K.J., Chen, D.S., Koeppen, H., 2011. Impact of exploratory biomarkers on the treatment effect of bevacizumab in metastatic breast cancer. Clinical Cancer Research 17, 372–381.

Katz-Brull, R., Seger, D., Rivenson-Segal, D., Rushkin, E., Degani, H., 2002. Metabolic markers of breast cancer: enhanced choline metabolism and reduced choline-ether-phospholipid synthesis. Cancer Research 62, 1966–1970.

Kerbel, R.S., 2009. Issues regarding improving the impact of antiangiogenic drugs for the treatment of breast cancer. Breast 18 (Suppl 3), S41–S47.

Lindholm, E.M., Kristian, A., Nalwoga, H., Kruger, K., Nygard, S., Akslen, L.A., Maelandsmo, G.M., Engebraaten, O., 2012. Effect of antiangiogenic therapy on tumor growth, vasculature and kinase activity in basal- and luminal-like breast cancer xenografts. Molecular Oncology 6, 418–427.

Mannelqvist, M., Stefansson, I.M., Bredholt, G., Hellem, B.T., Oyan, A.M., Jonassen, I., Kalland, K.H., Salvesen, H.B., Akslen, L.A., 2011. Gene expression patterns related to vascular invasion and aggressive features in endometrial cancer. American Journal of Pathology 178, 861–871.

Meisamy, S., Bolan, P.J., Baker, E.H., Bliss, R.L., Gulbahce, E., Everson, L.I., Nelson, M.T., Emory, T.H., Tuttle, T.M., Yee, D., Garwood, M., 2004. Neoadjuvant chemotherapy of locally advanced breast cancer: predicting response with in vivo (1)H MR spectroscopy–a pilot study at 4 T. Radiology 233, 424–431.

Milosevic, J., Maisel, M., Wegner, F., Leuchtenberger, J., Wenger, R.H., Gerlach, M., Storch, A., Schwarz, J., 2007. Lack of hypoxia-inducible factor-1 alpha impairs midbrain neural precursor cells involving vascular endothelial growth factor signaling. Journal of Neuroscience 27, 412–421.

Moestue, S.A., Borgan, E., Huuse, E., Lindholm, E., Sitter, B., Børresen-Dale, A.L., Engebråten, O., Maelandsmo, G., Gribbestad, I.S., 2010. Distinct choline metabolic profiles are associated with differences in gene expression for basal-like and luminal-like breast cancer xenograft models. BMC Cancer 10, 433.

Morse, D.L., Raghunand, N., Sadarangani, P., Murthi, S., Job, C., Day, S., Howison, C., Gillies, R.J., 2007. Response of choline metabolites to docetaxel therapy is quantified in vivo by localized (31)P MRS of human breast cancer xenografts and in vitro by high-resolution (31)P NMR spectroscopy of cell extracts. Magnetic Resonance in Medicine 58, 270–280.

Nishikawa, K.C., Millis, A.J., 2003. gp38k (CHI3L1) is a novel adhesion and migration factor for vascular cells. Experimental Cell Research 287, 79–87.

Oganesian, A., Armstrong, L.C., Migliorini, M.M., Strickland, D.K., Bornstein, P., 2008. Thrombospondins use the VLDL receptor and a nonapoptotic pathway to inhibit cell division in microvascular endothelial cells. Molecular Biology of the Cell 19, 563–571.

Paez-Ribes, M., Allen, E., Hudock, J., Takeda, T., Okuyama, H., Vinals, F., Inoue, M., Bergers, G., Hanahan, D., Casanovas, O., 2009. Antiangiogenic therapy elicits malignant progression of tumors to increased local invasion and distant metastasis. Cancer Cell 15, 220–231.

Podo, F., Canevari, S., Canese, R., Pisanu, M.E., Ricci, A., Iorio, E., 2011. MR evaluation of response to targeted treatment in cancer cells. NMR in Biomedicine 24, 648–672.

Rubenstein, J.L., Kim, J., Ozawa, T., Zhang, M., Westphal, M., Deen, D.F., Shuman, M.A., 2000. Anti-VEGF antibody treatment of glioblastoma prolongs survival but results in increased vascular cooption. Neoplasia 2, 306–314.

Saidi, A., Javerzat, S., Bellahcene, A., De, V.J., Bello, L., Castronovo, V., Deprez, M., Loiseau, H., Bikfalvi, A., Hagedorn, M., 2008. Experimental anti-angiogenesis causes upregulation of genes associated with poor survival in glioblastoma. International Journal of Cancer 122, 2187–2198.

Schneider, B.P., Sledge Jr., G.W., 2011. Anti-vascular endothelial growth factor therapy for breast cancer: can we pick the winners? Journal of Clinical Oncology 29, 2444–2447.

Schneider, B.P., Wang, M., Radovich, M., Sledge, G.W., Badve, S., Thor, A., Flockhart, D.A., Hancock, B., Davidson, N., Gralow, J., Dickler, M., Perez, E.A., Cobleigh, M., Shenkier, T., Edgerton, S., Miller, K.D., 2008. Association of vascular endothelial growth factor and vascular endothelial growth factor receptor-2

genetic polymorphisms with outcome in a trial of paclitaxel compared with paclitaxel plus bevacizumab in advanced breast cancer: ECOG 2100. Journal of Clinical Oncology 26, 4672–4678.

Sitter, B., Sonnewald, U., Spraul, M., Fjosne, H.E., Gribbestad, I.S., 2002. High-resolution magic angle spinning MRS of breast cancer tissue. NMR in Biomedicine 15, 327–337.

Smith, I., Pierga, J.Y., Biganzoli, L., Cortes-Funes, H., Thomssen, C., Saracchini, S., Nisenbaum, B., Pelaez, I., Duenne, A.A., Pritchard, K.I., 2011. Final overall survival results and effect of prolonged (>/=1 year) first-line bevacizumab-containing therapy for metastatic breast cancer in the ATHENA trial. Breast Cancer Research Treatment 130, 133–143.

Smyth, G.K., 2011. Limma: linear models for microarray data. In: Gentleman, R., Carey, V., Dudoit, S., Irizarry, R., Huber, W. (Eds.), Bioinformatics and Computational Biology Solutions Using R and Bioconductor. Springer, New York, pp. 397–420.

Smyth, G.K., 2004. Linear models and empirical bayes methods for assessing differential expression in microarray experiments. Statistical Application in Genetics and Molecular Biology 3. Article3.

Smyth, G.K., Michaud, J., Scott, H.S., 2005. Use of within-array replicate spots for assessing differential expression in microarray experiments. Bioinformatics 21, 2067–2075.

Sotiriou, C., Wirapati, P., Loi, S., Harris, A., Fox, S., Smeds, J., Nordgren, H., Farmer, P., Praz, V., Haibe-Kains, B., Desmedt, C., Larsimont, D., Cardoso, F., Peterse, H., Nuyten, D., Buyse, M., Van, d. V., Bergh, J., Piccart, M., Delorenzi, M., 2006. Gene expression profiling in breast cancer: understanding the molecular basis of histologic grade to improve prognosis. Journal of the National Cancer Institute 98, 262–272.

Troyanskaya, O., Cantor, M., Sherlock, G., Brown, P., Hastie, T., Tibshirani, R., Botstein, D., Altman, R.B., 2001. Missing value estimation methods for DNA microarrays. Bioinformatics 17, 520–525.

Vargo-Gogola, T., Rosen, J.M., 2007. Modelling breast cancer: one size does not fit all. National Reviews Cancer 7, 659–672.

Von Minckwitz, G., Eidtmann, H., Rezai, M., Fasching, P.A., Tesch, H., Eggemann, H., Schrader, I., Kittel, K., Hanusch, C., Kreienberg, R., Solbach, C., Gerber, B., Jackisch, C., Kunz, G., Blohmer, J.U., Huober, J., Hauschild, M., Fehm, T., Muller, B.M., Denkert, C., Loibl, S., Nekljudova, V., Untch, M., 2012. Neoadjuvant chemotherapy and bevacizumab for HER2-negative breast cancer. The New England Journal of Medicine 366, 299–309.

Yang, S.X., Steinberg, S.M., Nguyen, D., Wu, T.D., Modrusan, Z., Swain, S.M., 2008. Gene expression profile and angiogenic marker correlates with response to neoadjuvant bevacizumab followed by bevacizumab plus chemotherapy in breast cancer. Clinical Cancer Research 14, 5893–5899.

Young, S.D., Hill, R.P., 1990. Effects of reoxygenation on cells from hypoxic regions of solid tumors: anticancer drug sensitivity and metastatic potential. Journal of the National Cancer Institute 82, 371–380.